Supplementary Information (SI) for Physical Chemistry Chemical Physics.

Supplemental Materials for

Physical insights into the high radiative cooling power of cellulose-based materials

Zhuo Zhao[a,b], Jian Zhang[b], Yuan Cheng[c,d], Aijun Hou[b], Yabei Xu[a], Daxin Liang[a,*], Gang Zhang[b,*]

[a] Key Laboratory of Bio-based Material Science & Technology (Ministry of Education), Northeast Forestry University, Harbin 150040, China

[b] Yangtze Delta Region Academy of Beijing Institute of Technology (Jiaxing), Jiaxing 314019, China

[c] Monash Suzhou Research Institute, Monash University, Suzhou 215000, China

[d] Department of Materials Science and Engineering, Monash University, Clayton VIC 3800, Australia

* Corresponding author. E-mail: daxin.liang@nefu.edu.cn; zhanggang@bitjx.edu.cn

This file includes:

1. Supplementary experimental note.
2. Supplementary characterization note.
3. Figure S1 to S4.

1. Preparation of CNCs film.

CNCs suspension was prepared by hydrolyzing cotton pulp fibers with sulfuric acid. Specifically, 10 g of cotton was cut into small pieces and crushed with a grinder. And 106.8 g of water and 201.2 g of 98% concentrated sulfuric acid were measured. The cotton was soaked for 15 min and stirred with a glass rod. The hydrolysis was vigorously stirred at 45 ° C for 45 minutes. The resulting light yellow slurry was then added to deionized water to prevent further hydrolysis. The transparent top layer of the suspension was discarded, and the turbid residue was transferred to a dialysis bag (3500-5000 molecular weight cutoff) and dialyzed at a low flow rate for 3-5 days until the pH of the water reached neutral. Finally, the milky white CNCs suspension was rotary evaporated to the desired concentration to prepare a cellulose nanocrystal film.

2.1 Optical performance simulation and testing.

The reflectivity of the membranes was measured by an Ultraviolet-visible Near Infrared (UV–VIS–NIR) spectrophotometer (Lambda-1050+, Perkin Elmer, USA). The measurements were conducted within the wavelength range of 250 - 2500 nm. The average solar reflectance in the full solar spectrum (250 - 2500 nm) can be calculated by equation S1:

$$\bar{R}_{\text{solar}} = \frac{\int_{0.25}^{2.5} I_{\text{solar}}(\lambda) R(\lambda) \mathrm{d}\lambda}{\int_{0.25}^{2.5} I_{\text{solar}}(\lambda) \mathrm{d}\lambda} \quad \text{(S1)}$$

where $I_{\mathrm{solar}}(\lambda)$ is the solar intensity spectrum at air mass (AM) 1.5, and $R(\lambda)$ is the spectral reflectance in the in the full solar spectrum.

The Infrared (IR) spectrometer (VERTEX 70, Bruker, USA) with an A562 integrating sphere was used to determine the MIR spectral reflectivity/emissivity of the membranes in the wavelength range of 2.5 - 25 μm.

According to Kirchhoff's law, $\varepsilon(T, \lambda)$ can be defined by equation S2:

$$\varepsilon = 1 - T - R \tag{S2}$$

where T is the transmittance and R is the reflectance in IR spectroscopy.

The average IR emittance in the atmospheric window (8 – 13 μm) can be calculated by equation S3:

$$\varepsilon_{8\text{ - }13\mu\mathrm{m}} = \frac{\int_{8}^{13} I_{\mathrm{BB}}(T,\lambda)\varepsilon(T,\lambda)\mathrm{d}\lambda}{\int_{8}^{13} I_{\mathrm{BB}}(T,\lambda)\mathrm{d}\lambda} \tag{S3}$$

where $I_{\mathrm{BB}}(T, \lambda)$ is the spectral intensity emitted by a standard blackbody with temperature, and $\varepsilon(T, \lambda)$ is the spectral emittance of a cooler.

2.2 Characterization of radiative cooling capacity.

The theoretical calculation equations for daytime radiative cooling power are as follows:

When the radiation cooling device is placed under the sun, the net cooling power P_{net} depends on the following equation:

$$P_{\mathrm{net}}(T) = P_{\mathrm{rad}}(T) - P_{\mathrm{atm}}(T_{\mathrm{amb}}) - P_{ab}^{visible} - P_{(\mathrm{cond\ +\ conv})} \tag{S4}$$

where, P_{rad} is the thermal outward radiative power by the radiative cooler. P_{atm} is the absorbed energy from atmospheric thermal radiation, P_{sol} is the absorbed incident solar radiation, and the $P_{\mathrm{cond+conv}}$ is the heat conduction-convection from ambient radiation.

Thermal outward radiative power (P_{rad}):

$$P_{\mathrm{rad}}(T) = \int \mathrm{d}\Omega \cos\theta \int_0^{\infty} \mathrm{d}\lambda I_{\mathrm{BB}}(T,\lambda)\varepsilon(\lambda,\theta) \tag{S5}$$

where, θ is the local zenith angle, I_{BB} (T,λ) is the intensity of the radiation wave at the real-time temperature and the wavelength generated by the blackbody. ε (λ,θ) is the emissivity of the material at the wavelength λ.

angular integral on the hemisphere:

$$I_{\mathrm{BB}}(T,\lambda) = \frac{2hc^2}{\lambda^5} \frac{1}{\mathrm{e}^{\frac{hc}{\lambda T k_B}} - 1} \tag{S6}$$

where T is spectral radiation temperature of blackbody, and h is Planck's constant. k_{B} is the Boltzmann constant, c is the speed of light, and λ is the wavelength.

Absorbed energy from atmospheric thermal radiation (P_{atm}):

$$P_{\mathrm{atm}}(T_{\mathrm{amb}}) = \int \mathrm{d}\Omega \cos\theta \int_0^{\infty} \mathrm{d}\lambda I_{\mathrm{BB}}(T_{\mathrm{amb}},\lambda)\varepsilon(\lambda,\theta)\varepsilon_{\mathrm{atm}}(\lambda,\theta) \tag{S7}$$

where T_{amb} is the ambient temperature, $\varepsilon_{\mathrm{atm}}$ (λ, θ) is the atmospheric emissivity at zenith angle θ and wavelength λ.

Absorbed incident solar radiation ($P_{ab}^{visible}$):

First, conventional visible light heat absorption calculations:

$$P_{\mathrm{ab}}^{\mathrm{visible}} = \int_0^{\infty} \mathrm{d}\lambda \in (\lambda,\theta_{\mathrm{ab}}) I_{\mathrm{AM1.5}}(\lambda) \tag{S8}$$

where $I_{\mathrm{AM1.5}}$ (λ) is the AM1.5 received standard solar spectral irradiation intensity and θ_{ab} is the inclination of the sample surface facing the sun.

Heat conduction-convection from ambient radiation ($P_{\mathrm{cond+conv}}$):

$$P_{\mathrm{cond+conv}}(T,T_{\mathrm{amb}}) = h_{\mathrm{cc}}(T_{\mathrm{amb}} - T) \tag{S9}$$

where h_{cc} is the non radiative heat transfer coefficient which, in low humidity climate, has a typical values comprised in the range 0 - 12 W m^{-2} K^{-1}.

3. Figures.

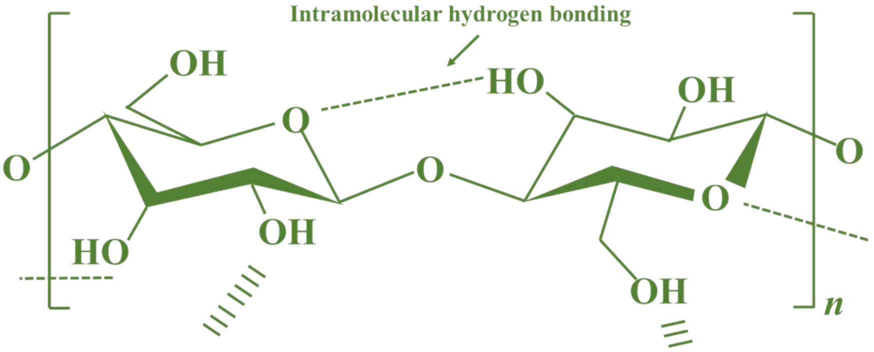

Figure S1. The molecular structure of cellulose.

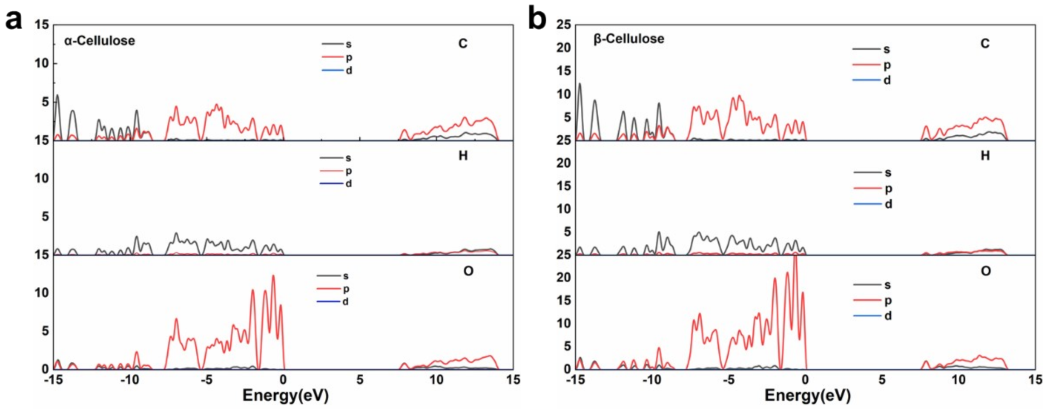

Figure S2. (a, b) The corresponding Projected DOS of cellulose I_{α} and I_{β}, respectively.

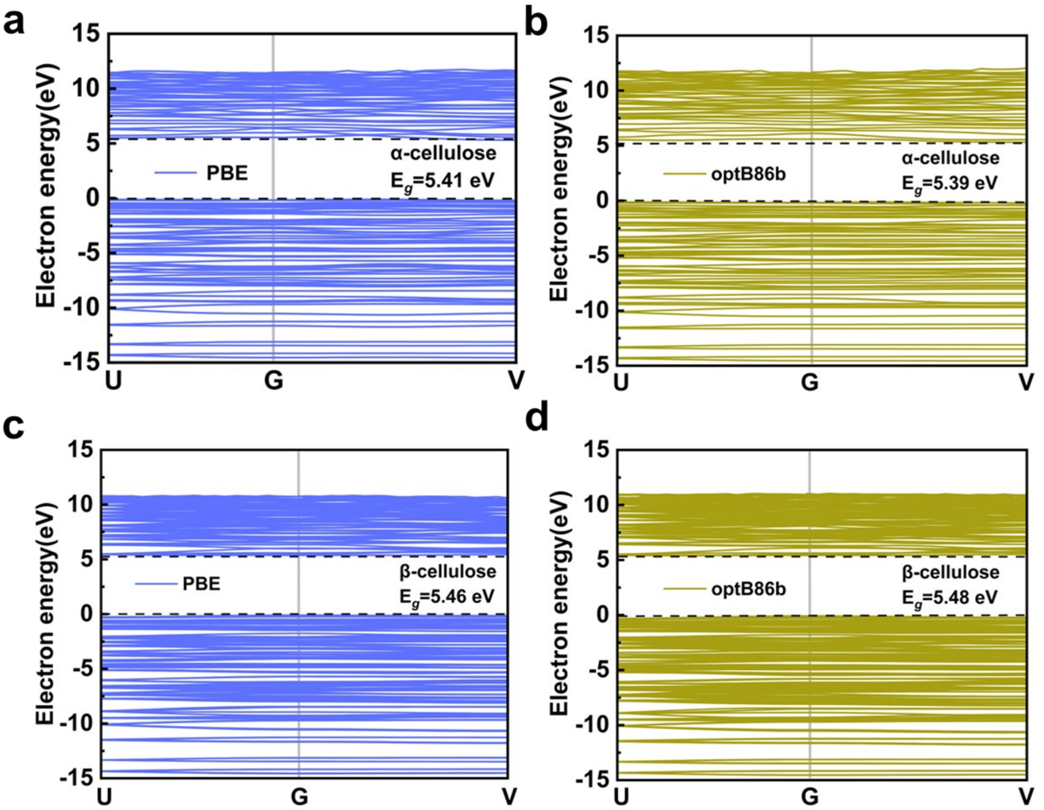

Figure S3. (a, c) Electronic energy bands based on PBE functional of cellulose I_α and I_β, respectively. (b, d) Electronic energy bands based on optB86b functional of cellulose I_α and I_β, respectively.

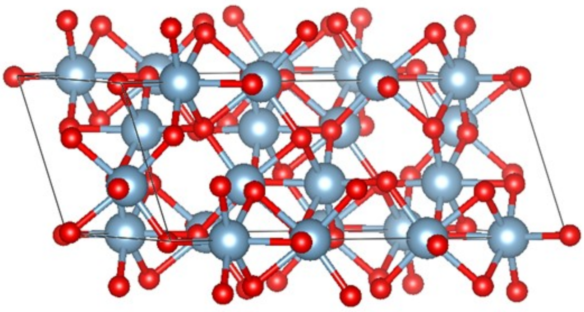

Figure S4. Crystal structure of unit cell of Al_2O_3.

Table S1. The optimized structural parameters of Al_2O_3[1].

Materials	Space group	a (Å)	b (Å)	c (Å)	α (°)	β (°)	ɣ (°)
Al_2O_3	$R\bar{3}c$	4.81	4.81	13.1	90.0	90.0	120

[1] L.W. Finger and R.M. Hazen. Crystal structure and compression of ruby to 46 kbar. Journal of Applied Physics, 49:5823–5826, 1978.

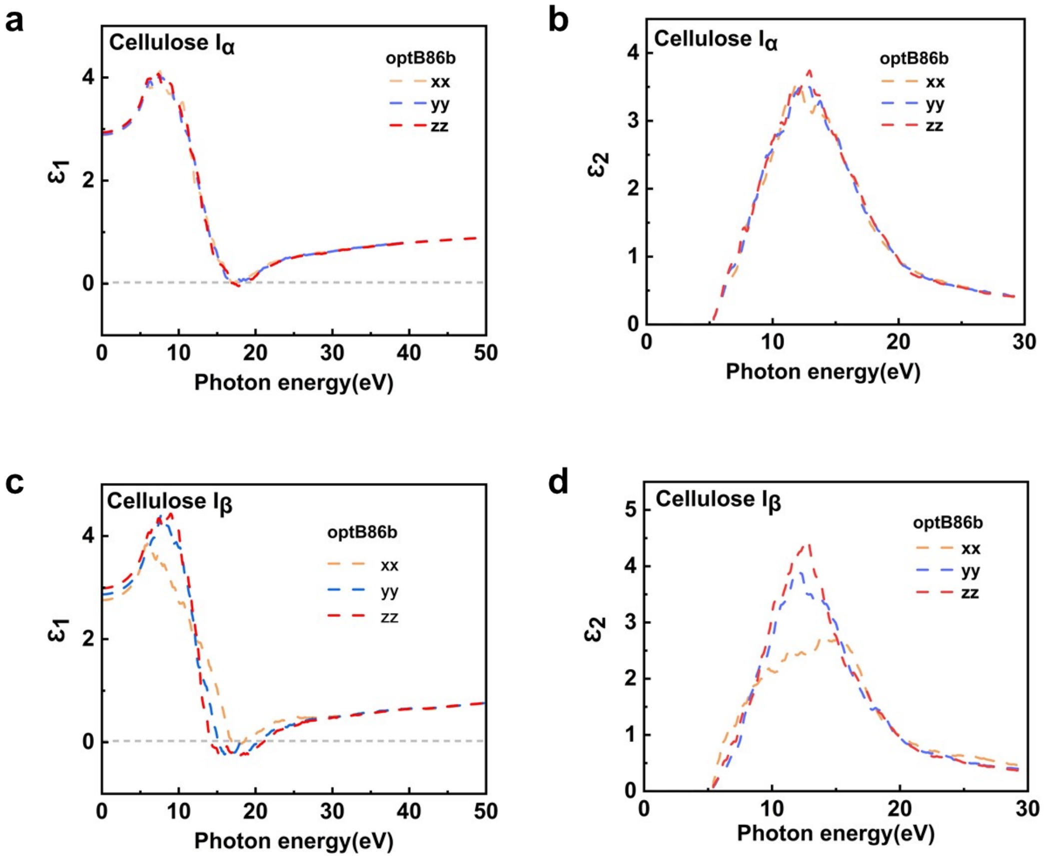

Figure S5. (a, b) The real and imaginary parts of the frequency-dependent dielectric function of cellulose I_α, respectively. (c, d) The real and imaginary parts of the frequency-dependent dielectric function of I_β, respectively.

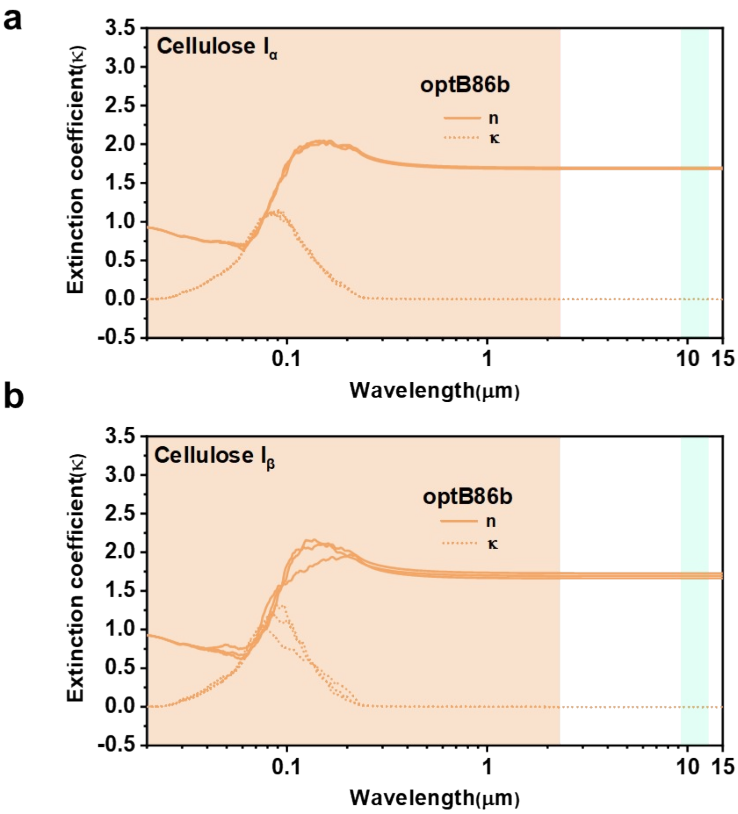

Figure S6. (a, b) The extinction coefficient of cellulose I_α and I_β based on optB86b functional, respectively.

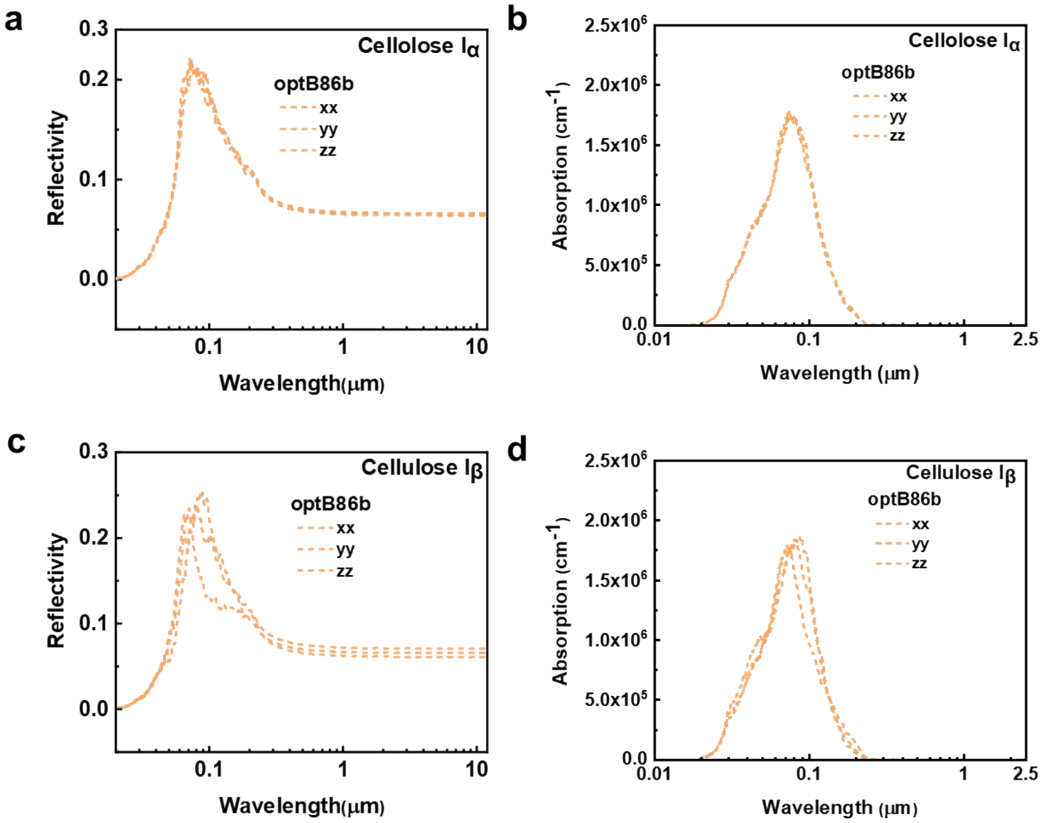

Figure S7. (a, b) Reflectivity and absorption of cellulose I_α, respectively. (c, d) Reflectivity and absorption of cellulose I_β, respectively.